THE PUBLISHING HOUSE
OF THE ROMANIAN ACADEMY

PROCEEDINGS OF THE ROMANIAN ACADEMY, Series A
Volume 26, Number 1/2025, pp. 75–87

DOI: 10.59277/PRA-SER.A.26.1.10

ROBUST NEUROADAPTIVE TRAJECTORY TRACKING FOR QUADROTOR UAV BASED ON NON-SINGULAR TERMINAL SLIDING MODE CONTROL

Yulin CHEN [1], Yuan LI [2], Zhidong WEN [3], Xiongbo BIE [4]

[1] Chongqing Industry Polytechnic College, 401120, China
[2] Wuhan Polytechnic, School of Mechanical and Electrical Engineering, 430072, China
[3] Yantai CAST Industrial Technology Research Institute Co., Ltd.,
No.67 Baiyunshan Road, Fushan District, 264000, China
[4] Chongqing Academy of Science and Technology for Development, 401120, China
Corresponding author: Xiongbo BIE, E-mail: kuailedexiaobie@163.com

Abstract. The quadrotor UAV is an underactuated, strongly coupled, and highly unstable nonlinear system. In order to address the issue of external interference during the actual flight of the quadrotor UAV and enhance the accurate trajectory tracking effect under system parameter perturbations, a trajectory tracking algorithm based on neural networks and terminal sliding mode control is designed. A non-singular neural network is utilized to approximate the unknown terms in the system. A low-pass filter is introduced to avoid differential operations and filter noise in the parameters. To ensure the robustness of the system, a terminal sliding mode controller is designed, and an adaptive parameter estimation method is developed to mitigate the system's chattering phenomenon. Consequently, the system state can track a given desired signal more accurately. The stability of the designed controller is proven using the Lyapunov stability theorem. Taking a quadrotor UAV as an example, the validity and reliability of the proposed method are verified through computer simulations.

Keywords: neural network, non-singularity, terminal sliding mode control (TSMC), trajectory tracking.

1. INTRODUCTION

In recent years, due to the high maneuverability and agility of quadrotor UAVs, they can complete vertical take-offs and landings, hovering in the air, low-speed cruising, and other flying tasks. They have been widely used in aerial surveying and mapping, military investigations, disaster monitoring, agricultural plant protection, and other fields. Trajectory tracking is the foundation for UAVs to complete specific tasks. Therefore, achieving high-precision UAV trajectory tracking has always been a hot topic of current research [1–3].

The quadrotor UAV is an underactuated system with four inputs and six outputs. There is a semi-coupling relationship between system variables, and there are non-holonomic constraints in the model, which complicates controller design. In actual use, it is impossible to construct an accurate mathematical model due to uncertain interferences from the external environment. At the same time, there are deviations between the system's measured values and the actual values of the UAV's mass, aerodynamic coefficients, moment of inertia, and other parameters, which further increases the difficulty of control [4–7].

To solve the above problems, many new methods have been proposed. For example, fuzzy logic [8, 9], backstepping [10], sliding mode control [11], and neural network control [12, 13] have been reflected in the

literature. Among them, sliding mode control technology boasts strong anti-interference ability and has been widely applied in UAV control and tracking. In [14], a second-order sliding mode controller is designed to track the height of the quadrotor aircraft, which reduces the chattering phenomenon compared to a first-order controller. For a quadrotor UAV with dynamic uncertainty, [15] designs a high-order sliding mode observer for trajectory tracking, and constructs a position loop compound nonlinear dynamic inverse controller and an attitude loop compound nonsingular terminal sliding mode controller. To eliminate the singularity problem of traditional terminal sliding mode control, [16] proposes a nonsingular terminal sliding mode controller, ensuring the system converges to the equilibrium point in finite time. To verify that the disturbance information of the quadrotor UAV is more aligned with actual conditions, [17] considers fuselage parameter disturbances and external disturbances, combining them with an uncertainty coefficient. By decoupling the dynamic model, position and attitude subsystems are obtained. The sliding mode control method based on a multi-dimensional Taylor network is employed to achieve accurate trajectory tracking. In [18], sliding mode control is utilized as an adaptive mechanism to overcome the gain re-adjustment issue in PID, and a fuzzy compensator is introduced to eliminate chattering.

Recent advancements in data-driven control techniques have shown significant promise in enhancing the performance of sliding mode control (SMC) for disturbance rejection. Data-driven sliding mode control (DDSMC) leverages real-time system data to adaptively adjust control strategies, particularly in the presence of unknown disturbances and system uncertainties. Unlike traditional model-based approaches, DDSMC does not rely heavily on precise system models, making it highly suitable for complex and uncertain systems such as quadrotor UAVs. For instance, [19] proposed a data-driven sliding mode control framework that combines machine learning techniques with SMC to improve disturbance rejection capabilities. Similarly, [20, 21] developed an adaptive data-driven SMC approach that uses online learning to estimate and compensate for external disturbances in real-time. These methods have demonstrated superior performance in handling uncertainties and external disturbances, making them a valuable addition to the existing control strategies for UAVs.

Neural network technology has been extremely popular in recent years. Its nonlinear structure is often used to approximate unknown functions in control systems and serve as a compensator. When the model of a quadrotor UAV is uncertain or subject to unknown disturbances, neural networks are widely employed to address these issues, enabling the controller to track effectively and swiftly. In the work presented in [22], an adaptive radial basis function neural network is used to approximate the unknown term in the model, thereby obviating the need for an accurate dynamic model and disturbance prior information. In [23], adaptive neural networks and sliding mode control are combined, where the sliding mode controller is used to design the subsystems, and the neural network is used to adjust the coefficients within the sliding mode controller. In the fault-tolerant tracking system of UAVs, [24] designs a radial basis function neural network to identify model uncertainties online adaptively and modify the reference model accordingly.

In this paper, we design a neural network Non-singular terminal sliding mode control for trajectory tracking. The overall control of quadrotor UAV is shown in Fig. 1. Compared with the above-mentioned methods in the existing literature, the main contributions of this paper are as follows:

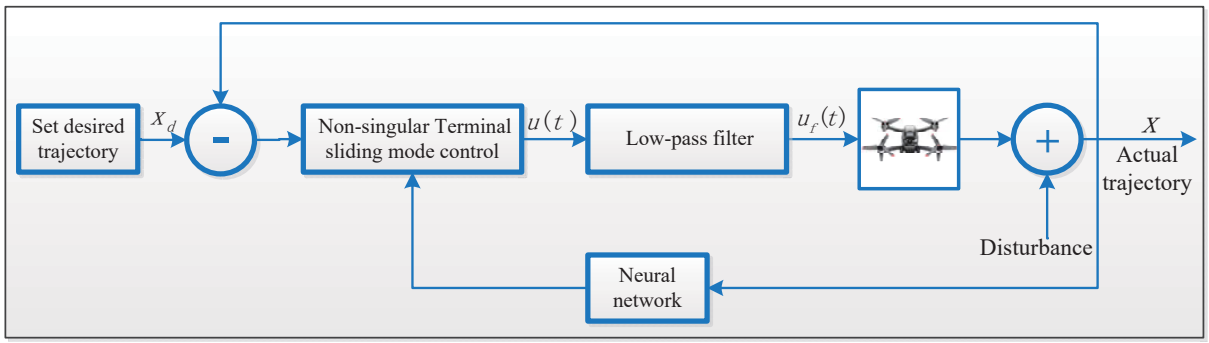

Fig. 1 – Overall structure block diagram of the algorithm.

1. The original dynamic equation is transformed into a new form with unit control gain, the singular point problem is solved, and the neural network is used to approximate the lumped unknown nonlinear term.
2. Introducing a low-pass filter to process signals such as states and controllers reduces the amplitude of noise and improves the stability of algorithm design.
3. The terminal sliding mode controller is used to replace the traditional sliding mode controller, and its nonlinear characteristics increase the flexibility of algorithm design and solve the chattering situation.

The outline of this article is organized as follows. In Section 2, the mathematical model of a quadrotor UAV is established. Section 3 design a non-singular neural network control. Neural network terminal sliding mode control is given in Section 4. Simulation results are given in Section 5 to demonstrate the effectiveness of the proposed algorithm. Finally, Section 6 concludes this article.

2. DYNAMIC MODEL OF QUADROTOR UAV

In this article, we consider the dynamic model of the quadrotor UAV system and its model derivation process. The actual quadrotor UAV is shown in Fig. 2. The fuselage coordinate system and the earth coordinate system are defined as $B(x_b, y_b, z_b)$, $E(x_e, y_e, z_e)$ respectively.

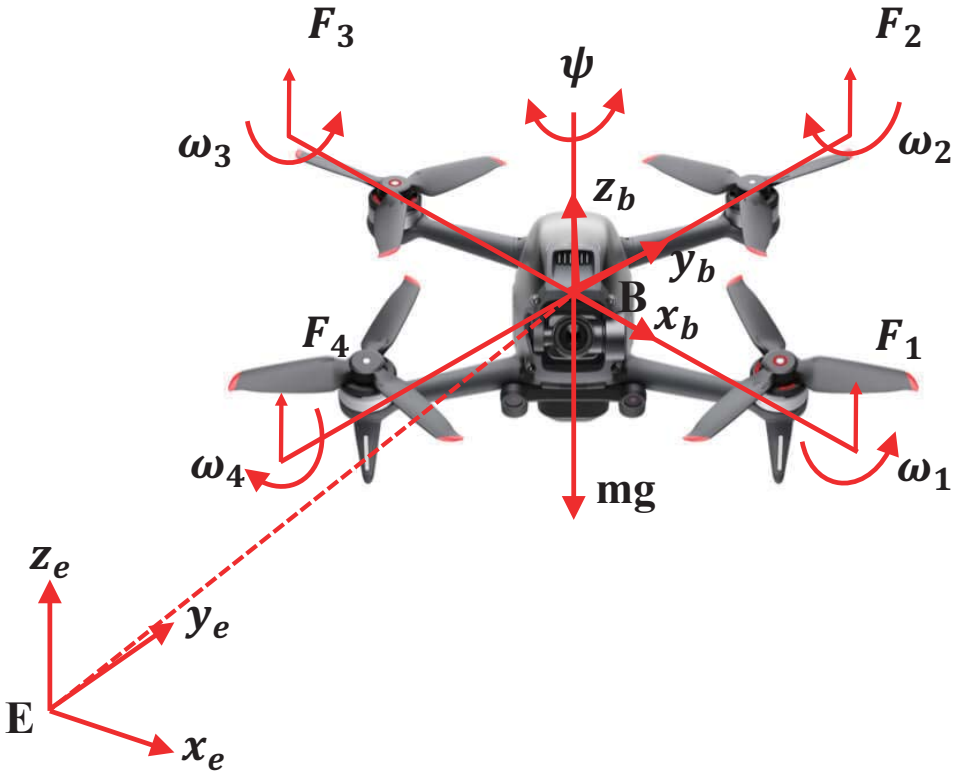

Fig. 2 – Quadrotor UAV model structure.

To simplify the quadrotor UAV system and facilitate the calculation, the system model is assumed as follows:

1. The fuselage of quadrotor UAV is rigid and strictly symmetrical;
2. There is no deformation and galloping of the propeller;
3. The origin of the body coordinate system coincides with the center of mass of the UAV.

The linear velocity and angular velocity defined by the UAV in the fuselage coordinate system are $\mathbf{V} = [u,v,w]^T \in \mathbb{R}^3$ and $\Omega = [p,q,r]^T \in \mathbb{R}^3$, respectively. The displacement and Euler angle of the UAV in the earth coordinate system are $\xi = [x,y,z]^T \in \mathbb{R}^3$ and $\eta = [\varphi,\theta,\psi]^T \in \mathbb{R}^3$, where φ, θ, and ψ are the roll angle, pitch angle, and yaw angle, respectively. The relationship between the two coordinate systems can be expressed as:

$$\begin{aligned} \dot{\xi} &= JV, \\ \dot{\eta} &= K\Omega \end{aligned} \tag{1}$$

where $\mathbf{J} \in \mathbb{R}^{3\times3}$ and $\mathbf{K} \in \mathbb{R}^{3\times3}$ are transformation matrices defined as:

$$J = \begin{bmatrix} C\psi C\theta & C\psi S\theta S\varphi - S\psi C\varphi & C\psi S\theta C\varphi + S\psi S\varphi \\ S\psi C\theta & S\psi S\theta S\varphi + C\psi C\varphi & S\psi S\theta C\varphi - C\psi S\varphi \\ -S\theta & \cos\theta S\varphi & C\theta C\varphi \end{bmatrix} \tag{2}$$

$$V = b\sum_{i=1}^{4}\omega_i^2, i = 1,2,3,4 \tag{3}$$

$$K = \begin{bmatrix} 1 & S\varphi T\theta & C\varphi T\theta \\ 0 & C\varphi & -S\varphi \\ 0 & S\varphi/C\theta & C\varphi/C\theta \end{bmatrix} \tag{4}$$

where, $S = \sin(\cdot)$, $C = \cos(\cdot)$, and $T = \tan(\cdot)$. According to Newton-Euler equations, the dynamic equation of quadrotor UAV is obtained as follows:

$$\begin{aligned} m\ddot{\xi} &= \begin{bmatrix} 0 \\ 0 \\ -mg \end{bmatrix} + J\begin{bmatrix} 0 \\ 0 \\ V \end{bmatrix}, \\ I\dot{\Omega} + \Omega \times I\Omega &= M^B \end{aligned} \tag{5}$$

where, $\mathbf{M}^B \in \mathbb{R}^3$ is the control torque.

$$M^B = \begin{bmatrix} b & b & b & b \\ 0 & -db & 0 & db \\ -db & 0 & db & 0 \\ k & -k & k & -k \end{bmatrix} + \begin{bmatrix} \omega_1^2 \\ \omega_2^2 \\ \omega_3^2 \\ \omega_4^2 \end{bmatrix} \tag{6}$$

where, $\Omega \times I\Omega$ is gyro moment. d is the distance between the quadrotor center of mass and the axis of the propeller and k is the drag factor. $\mathbf{I} \in \mathbb{R}^{3\times3}$ is the inertia matrix of quadrotor aircraft under stable structure, which is expressed as follows:

$$I = \begin{bmatrix} I_x & 0 & 0 \\ 0 & I_y & 0 \\ 0 & 0 & I_z \end{bmatrix} \tag{7}$$

where I_x, I_y, and I_z are the inertia of x, y and z axes respectively. After being brought into the system, the UAV

dynamic model can be expressed as follows:

$$\begin{aligned}
\dot{x} &= \frac{(S\varphi S\varphi + C\phi C\psi S\theta)V}{m}, \\
\dot{y} &= \frac{(C\varphi S\psi S\theta - C\psi S\varphi)V}{m}, \\
\dot{z} &= \frac{(C\varphi C\theta)V - mg}{m}, \\
\dot{p} &= \frac{-\dot{\theta}\dot{\psi}(I_z - I_y) + M_x^B}{I_x}, \\
\dot{q} &= \frac{-\dot{\varphi}\dot{\psi}(I_x - I_z) + M_y^B}{I_y}, \\
\dot{r} &= \frac{-\dot{\theta}\dot{\varphi}(I_y - I_x) + M_z^B}{I_z}
\end{aligned} \tag{8}$$

$$\begin{bmatrix} M_x^B \\ M_y^B \\ M_z^B \end{bmatrix} = \begin{bmatrix} db(\omega_4^2 - \omega_2^2) \\ db(\omega_3^2 - \omega_1^2) \\ k(\omega_1^2 + \omega_3^2 - \omega_2^2 - \omega_4^2) \end{bmatrix} \tag{9}$$

The input of UAV is

$$\begin{aligned}
U_1 &= b(\omega_1^2 + \omega_2^2 + \omega_3^2 + \omega_4^2) \\
U_2 &= db(\omega_4^2 - \omega_2^2) \\
U_3 &= db(\omega_3^2 - \omega_1^2) \\
U_4 &= k(\omega_1^2 - \omega_2^2 + \omega_3^2 - \omega_4^2)
\end{aligned} \tag{10}$$

where,ω_1, ω_2, ω_3, and ω_4 are expressed as the speed of four motors of UAV. b is a positive constant called thrust factor.

3. NON-SINGULAR NEURAL NETWORK CONTROL

When the quadrotor UAV considers external interference, the nonlinear dynamic equation can be simplified as

$$\ddot{x} = f(x) + g(x)u + d \tag{11}$$

where $\mathbf{x} = [Z, \varphi, \theta, \psi]^T \in \mathbb{R}^4$ is the state vector, $Z(t) \in \mathbb{R}$ is the altitude of the quadrotor, $\mathbf{f}(\mathbf{x}) \in \mathbb{R}^4$ is an unknown continuous nonlinear function, $\mathbf{g}(\mathbf{x}) \in \mathbb{R}^{4\times4}$ is an unknown continuous nonlinear function matrix satisfying $\mathbf{g}(\mathbf{x}) > 0$, $\mathbf{u} = [u_1, u_2, u_3, u_4]^T \in \mathbb{R}^4$ represents the control input vector, and $\mathbf{d} = [d_1, d_2, d_3, d_4]^T \in \mathbb{R}^4$ represents the external disturbance vector with $|d_i| \leq \delta$, $i = 1,2,3,4$, where $\delta \in \mathbb{R}$ is a positive constant. To design an adaptive controller for (11), a novel non-singular neural network control algorithm is proposed.

Considering the nonlinear system of (11), the original formula can be rewritten as

$$c^*\ddot{x} = c^* f(x) + u + \zeta_1 \tag{12}$$

where $c^* = 1/g(x)$ and $\zeta_1 = c^* d$. Using NNs to approximate c^* and $c^* f(x)$ as

$$c^* f(x) = w^* \phi + \zeta_2 \tag{13}$$

where $\mathbf{W}^* = [\mathbf{w}_1^*, \ldots, \mathbf{w}_n^*] \in \mathbb{R}^{4\times n}$ is the ideal weight matrix for the neural network, $\boldsymbol{\phi} = [\phi_1, \ldots, \phi_n]^T \in \mathbb{R}^n$ is the basis vector for the neural network, and $\boldsymbol{\zeta}_2 \in \mathbb{R}^4$ is the sum of the approximation error and external disturbance,

satisfying $|\zeta_2| \leq \zeta_{2N}$, where $\boldsymbol{\zeta}_{2N} \in \mathbb{R}^4$ is a positive constant vector. $n \in \mathbb{N}$ is the number of neurons. Therefore, (12) can be rewritten as

$$u = c^* \ddot{x} - w^* \phi - \zeta_3 \tag{14}$$

where $\zeta_3 = \zeta_1 + \zeta_2$ is the combination error. Define a stable low-pass filter $G = 1/(\lambda s + 1)$ to $\dot{x}$, u, ϕ, and ζ_3, filtered variable $\dot{\mathbf{x}}_f \in \mathbb{R}^4$, $\mathbf{u}_f \in \mathbb{R}^4$, $\boldsymbol{\phi}_f \in \mathbb{R}^n$, and $\boldsymbol{\zeta}_{3f} \in \mathbb{R}^4$ are introduce as

$$\dot{x}_f = \frac{\dot{x}}{\lambda s + 1} \Leftrightarrow \lambda \ddot{x}_f + \dot{x}_f = \dot{x} \tag{15}$$

$$u_f = \frac{u}{\lambda s + 1} \Leftrightarrow \lambda \dot{u}_f + u_f = u \tag{16}$$

$$\phi_f = \frac{\phi}{\lambda s + 1} \Leftrightarrow \lambda \dot{\phi}_f + \phi_f = \phi \tag{17}$$

$$\zeta_{3f} = \frac{\zeta_3}{\lambda s + 1} \Leftrightarrow \lambda \dot{\zeta}_{3f} + \zeta_{3f} = \zeta_3 \tag{18}$$

where $\phi_f(0) = 0$ and $\zeta_{3f}(0) = 0$. λ is a filter parameter, and $\lambda \geq 0$. Therefore, (14) can be rewritten as

$$u_f = c^* \ddot{x}_f - w^* \phi_f - \zeta_{3f} := W\Phi - \zeta_{3f} \tag{19}$$

where $W = [c^*, -w^*]$ and $\Phi = [\ddot{x}_f; \phi_f]$. For (14), we use the following neural network to estimate it

$$\hat{u} = \hat{c} \ddot{x}_f - \hat{w}^* \phi_f := \hat{W}\Phi \tag{20}$$

where $\hat{w}$ and $\hat{c}$ is expressed as an estimate of w^*, c^*, respectively. $\hat{W} = [\hat{c}, -\hat{w}^*]$, $\Phi = [\ddot{x}_f; \phi_f]$. Define the estimation error as

$$e_u = u_f - \hat{u} \tag{21}$$

Combine (19), (20) and (21) to obtain

$$e_u = \tilde{W}\Phi(x) - \zeta_{3f} \tag{22}$$

Where $\tilde{W} = W - \hat{W}$ is the weight estimation error. $| \zeta_{3f} | \leq \zeta_{3N}$, ζ_{3N} is a positive constant. The update rate $\hat{W}$ can be expressed as

$$\dot{\hat{W}} = \Gamma(\frac{\Phi^T e_u}{m} - \sigma \hat{W}) \tag{23}$$

where $m = \Delta + \Phi^T \Phi$.

THEOREM 1. *Consider the filtered nonlinear control system (12) and neural network estimation (13) of the quadrotor UAV. By using the update rate (23), the parameters $\hat{w}$ and $\tilde{W}$ satisfy uniformly ultimately bounded (UBB), and $\tilde{W}$ converges to a residual set around 0 exponentially.*

Proof. Consider the following candidate Lyapunov function

$$V_1 = \frac{1}{2\Gamma} \tilde{W} \tilde{W}^T \tag{24}$$

Combining (22) and (23), the derivative of the above formula can be expressed as

$$\begin{aligned} \dot{V}_1 &= -\tilde{W}(\frac{\Phi e_u}{m} - \sigma \hat{W}^T) \\ &= \frac{e_u}{m}(e_u + \zeta_{3f}) + \sigma \tilde{W}(W^T - \tilde{W}^T) \end{aligned} \tag{25}$$

Use the following inequality to simplify (25)

$$\tilde{W} W^T \leq \frac{\tilde{W}\tilde{W}^T}{2} + \frac{W W^T}{2} \tag{26}$$

$$-e_u\zeta_{3f} \leq \frac{e_u^2}{2} + \frac{\zeta_{4N}^2}{2} \tag{27}$$

Then (25) can be rewritten as

$$\begin{aligned} \dot{V}_1 &\leq \frac{\sigma}{2}WW^T + \frac{\zeta_{3N}^2}{2m} - \frac{e_u^2}{2m} - \frac{\sigma}{2}\tilde{W}\tilde{W}^T \\ &\leq -\sigma\Gamma V_1 + \frac{\sigma}{2}WW^T + \frac{\zeta_{3N}^2}{2\Delta} \\ &\leq -\eta V_1 + \varsigma \end{aligned} \tag{28}$$

where $\eta = \sigma\Gamma$ and $\varsigma = \frac{\sigma}{2}WW^T + \frac{\zeta_{3N}^2}{2\Delta}$. In order to make $\dot{V}_1 \leq 0$, just set $V_1 \geq (1/2\sigma\Gamma)((\zeta_{3N}^2/\Delta) + \sigma WW^T)$. According to Lyapunov's theorem, we know that $\tilde{W}$ is UBB, so we know that $\hat{w}_1$, $\hat{w}_2$, and $\hat{w}_3$ are bounded. Then, integrate (28) to get

$$\begin{aligned} V_1 &= \frac{1}{2\Gamma}\tilde{W}(t)\tilde{W}^T(t) \\ &\leq \frac{e^{-\sigma\Gamma t}}{2\Gamma}\tilde{W}(0)\tilde{W}^T(0) + \frac{1}{2\sigma\Gamma}(\sigma WW^T + \frac{\zeta_{3N}^2}{\Delta}) \end{aligned} \tag{29}$$

which means $\tilde{W}$ exponent converges to a compact residual set.

$$\Omega = \{\tilde{W} \mid \|\tilde{W}\| \leq \frac{\zeta_{3N}^2}{\Delta} + \| W \|\} \tag{30}$$

where $\| \cdot \|$ mean L_2 norm. Theorem 1 is thus proved. □

Remark 1. The Non-singular neural network control for quad-rotor drones proposed in this section mainly has the following two advantages:

1. The non-singularity method is used to process the nonlinear system. In (1), for the unknown control signal $g(x)$, in order to obtain the estimated $\hat{g}(x)$ of g(x) in the traditional method, a neural network feedback controller is often designed. Since $\hat{g}(x)^{-1}$ appears in the controller function, when $\hat{g}(x)^{-1}$ is very small or equal to zero, singularity problems will occur.This paper uses a non-singular neural network to estimate $\hat{g}(x)^{-1}$ to solve the singularity problem.
2. A low-pass filter is introduced to filter the noise of the measured signal. The measured signal often contains high-frequency noise during the acquisition process, and direct differentiation operation on it will increase the noise density, which will affect the stability of the system. In this paper, the low-pass filter used in (8-13) will weaken high-frequency noise and improve the robustness and stability of the system.

4. NEURAL NETWORK TERMINAL SLIDING MODE CONTROL

4.1. Controller design

The goal of the controller design is to minimize the trajectory tracking error of the system under the conditions of estimation error and external interference. The tracking error is defined as

$$e = x - x_d \tag{31}$$

where x_d is the desired trajectory of the system. In order to achieve the minimum steady-state error and achieve the desired trajectory convergence, this section adopts terminal sliding mode control, it is more flexible than traditional sliding mode control. Choosing the sliding surface as

$$k = \dot{e} + \beta e^{\frac{h}{n}} \tag{32}$$

where, h,n is positive odd, and satisfy $h < n < 2h$. β is a user-defined constant. Take the derivative of k can obtain

$$\begin{aligned} c^*\dot{k} &= c^*(\ddot{e} + \beta\frac{h}{n}e^{\frac{h}{n}-1}\dot{e}) \\ &= c^*\ddot{x} - c^*\ddot{x}_d + c^*\beta\frac{h}{n}e^{\frac{h}{n}-1}\dot{e} \\ &= w^*\phi + u + \zeta_3 - c^*\ddot{x}_d + c^*\beta\frac{h}{n}e^{\frac{h}{n}-1}\dot{e} \end{aligned} \tag{33}$$

Let $\dot{k} = 0$ and $\zeta_5 = 0$, using neural network regressor for unknown systems, the equivalent control can be obtained

$$u_{eq} = \hat{c}(\ddot{x}_d - \beta\frac{h}{n}e^{\frac{h}{n}-1}\dot{e}) - \hat{w}^*\phi \tag{34}$$

In order to compensate the total interference ζ_5 and the residual error between the training neural network and the ideal network, a switch control input is designed as

$$u_s = -\frac{L}{g}D^{\beta}sgn(k) \tag{35}$$

where L is a positive constant, sgn is the signum function of the sliding surface. The tracking error can be converged to zero by selecting an appropriate value of L.

THEOREM 2. Through the following combined control law, the terminal sliding mode function and the system tracking error will converge in a compact set around zero.

$$\begin{aligned} u &= u_{eq} + u_s \\ &= \hat{c}(\ddot{x}_d - \beta\frac{h}{n}e^{\frac{h}{n}-1}\dot{e}) - \hat{w}^*\phi - \frac{L}{g}D^{\beta}sgn(k) \end{aligned} \tag{36}$$

where $L \geq \zeta_{3N}$.

Proof. In order to verify the stability of the combined control law, the following candidate Lyapunov function is designed as

$$V_2 = V_1 - \frac{c^*}{2}k^2 \tag{37}$$

Through (33) and (36), the derivative of V_2 can be obtained as

$$\begin{aligned} \dot{V}_2 &= \dot{V}_1 + kc^*\dot{k} \\ &= \dot{V}_1 + k(w^*\phi + u + \zeta_3 - c^*\ddot{x}_d + c^*\beta\frac{h}{n}e^{\frac{p}{q}-1}\dot{e}) \\ &= \dot{V}_1 + k\{w^*\phi + \hat{c}(\ddot{x}_d - \beta\frac{h}{n}e^{\frac{h}{n}-1}\dot{e}) - \hat{w}\phi \\ &- \frac{L}{g}D^{\beta}sgn(k) + \zeta_3 - c^*\ddot{x}_d + c^*\beta\frac{h}{n}e^{\frac{h}{n}-1}\dot{e}\} \\ &= \dot{V}_1 + k(\zeta_3 + \tilde{W}\Xi - \frac{L}{g}D^{\beta}sgn(k)) \end{aligned} \tag{38}$$

where $\tilde{W} = [\tilde{c}, -\tilde{w}]$, $\Xi = [\beta\frac{h}{n}e^{\frac{h}{n}-1}\dot{e} - \ddot{x}_d; -\phi]$. Note that Ξ is bounded for a quadrotor UAV system, and $\|\Xi\| \leq \tau$, τ is a positive constant. From Young's inequality

$$k\tilde{W}\Xi \leq \frac{\tau}{2}k^2 + \frac{\tau}{2}\tilde{W}\tilde{W}^T = \frac{\tau}{2}k^2 + \tau\Gamma V_1 \tag{39}$$

Then (38) can be rewritten as

$$\begin{aligned}\dot{V}_2 &\leq -(\eta-\tau\Gamma)V_1+\frac{\tau}{2}k^2+\psi+k(\zeta_3-\frac{L}{g}D^{\beta}sgn(k))\\ &\leq -\eta_2 V_2+\varsigma+k(\zeta_3-\frac{L}{g}D^{\beta}sgn(k))\end{aligned} \tag{40}$$

where $\eta_2=\min\{\eta-\tau\Gamma,\frac{-\tau\Gamma}{c^*}\}$.By choosing a suitable L, such as $L\geq\zeta_{3N}$, so that $\dot{V}_2\leq-\eta_2V_2+\varsigma$. Through the integral operation we can get that,

$$V_2(t)=e^{-\eta_2 t}+\frac{\varsigma}{\eta_2} \tag{41}$$

The above formula shows that the $V_2(t)$ converges to a small residual approximation error exponentially, and the neural network estimation error and the system tracking error index converge to a compact set of zero. Theorem 2 is thus proved. □

4.2. Adaptive parameter estimation

In Theorem 2, $L\geq\zeta_{3N}$, in order to ensure the robustness of the system to external uncertain interference and approximation error, L often takes a large value, but this conservative method will lead to the deterioration of the system chattering and tracking performance.

This section uses an adaptive estimation method to calculate L, which has solved the above problems.

THEOREM 3. *Through the following adaptive control law, the terminal sliding mode function and the system tracking error will converge in a compact set around zero.*

$$u=\hat{c}(\ddot{x}_d-\beta\frac{h}{n}e^{\frac{h}{n}-1}\dot{e})-\hat{w}^*\phi-\frac{\hat{L}}{g}D^{\beta}sgn(k) \tag{42}$$

The adaptive control law of parameter L is written as

$$\dot{\hat{L}}=\rho(k+|k|) \tag{43}$$

where ρ is the adaptive gain.

Proof. In order to verify the stability of the adaptive control law, the following candidate Lyapunov function is designed as

$$V_3=V_2+\frac{1}{2\rho}\tilde{L}^2 \tag{44}$$

where $\tilde{L}=\hat{L}-L$. Combining (40) and (43), the derivative of V_3 can be expressed as

$$\begin{aligned}\dot{V}_3&=-\eta_2V_2+\varsigma+k(\zeta_3-\frac{\hat{L}}{g}D^{\beta}sgn(k))+\rho^{-1}\tilde{L}\dot{\hat{L}}\\ &=-\eta_2V_2+\varsigma+k(\zeta_3-\frac{\hat{L}}{g}D^{\beta}sgn(k))+\tilde{L}k+\tilde{L}|k|\end{aligned} \tag{45}$$

Let $|k|=\frac{k}{g}D^{\beta}sgn(k)$, can be deduced that

$$k(\zeta_3-\frac{\hat{L}}{g}D^{\beta}sgn(k))+\tilde{L}|k|=k(\zeta_3-\frac{L}{g}D^{\beta}sgn(k)) \tag{46}$$

From Young's inequality

$$\tilde{L}k\leq\frac{1}{2}(\tilde{L}^2+k^2) \tag{47}$$

Then (44) can be rewritten as

$$\begin{aligned}\dot{V}_3 &\leq -\eta_2 V_2 + \varsigma + k(\zeta_3 - \frac{L}{g} D^{\beta} sgn(k)) + \frac{1}{2}(\tilde{L}^2 + k^2) \\ &\leq -\eta_3 V_3 + \varsigma + k(\zeta_3 - \frac{L}{g} D^{\beta} sgn(k))\end{aligned} \tag{48}$$

where $\eta_3 = \min\{\eta_2, -\rho, \eta_2 - \frac{1}{c^*}\}$. Therefore, when $L \geq \zeta_{3N}$, (48) can be simplified to $\dot{V}_3 \leq -\eta_3 V_3 + \psi$. Through the integral operation we can get that,

$$V_3(t) = e^{-\eta_3 t} + \frac{\varsigma}{\eta_3} \tag{49}$$

This shows that $V_3(t)$ converges to a small residual approximation error exponentially. Theorem 3 is thus proved. □

Finally, the compound control law u can be expressed as

$$u = \hat{c}(\ddot{x}_d - \beta \frac{h}{n} e^{\frac{h}{n}-1} \dot{e}) - \frac{\hat{L}}{g} D^{\beta} sgn(k) - \hat{w}^* \phi \tag{50}$$

where u_{tsmc} and u_{nn} represent the control signals generated by adaptive terminal sliding mode controller and neural network controller respectively.

5. SIMULATION

In this section, we conduct simulations to demonstrate the effectiveness of the proposed neural network-based terminal sliding mode control (NN-TSMC) strategy for quadrotor UAV trajectory tracking. The simulations are designed to showcase the robustness of the proposed method under various uncertainties and constraints. The system and parameter settings involved in the simulations are consistent with those in Literature [25].

5.1. System description and simulation setup

The quadrotor UAV system is modeled with the following parameters: mass $m = 1\,\text{kg}$, thrust factor $b = 0.1$, drag factor $k = 1$, gravitational acceleration $g = 9.8\,\text{m/s}^2$, and filter parameter $\lambda = 0.01$. The desired trajectory is set as $x_d = \sin(t)$, which represents a sinusoidal path for the UAV to track.

To simulate realistic conditions, we introduce bounded external disturbances $d = [d_1, d_2, d_3, d_4]^T$, where $|d_i| \leq \delta$ for $i = 1, 2, 3, 4$, and $\delta = 0.5$. Additionally, we consider parameter uncertainties in the mass and moment of inertia, with deviations of up to 10% from the nominal values.

5.2. Simulation results and discussion

The simulation results are presented in Figs. 3–6. Fig. 3 shows the system's tracking of the desired trajectory. It can be observed that the proposed NN-TSMC strategy effectively tracks the desired trajectory despite the presence of external disturbances and parameter uncertainties.

Figure 4 displays the tracking error, which remains relatively small throughout the simulation. This demonstrates the robustness of the proposed control strategy in maintaining accurate trajectory tracking under uncertain conditions.

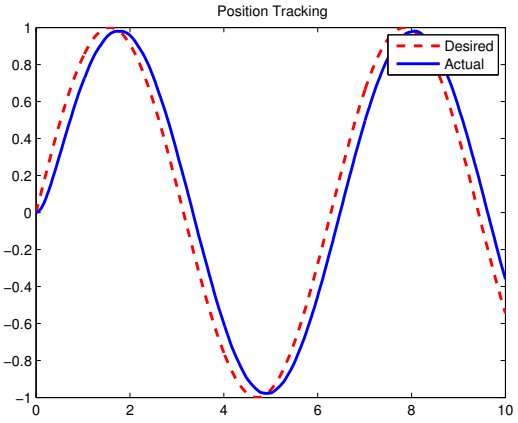

Fig. 3 – This is system tracking trajectory.

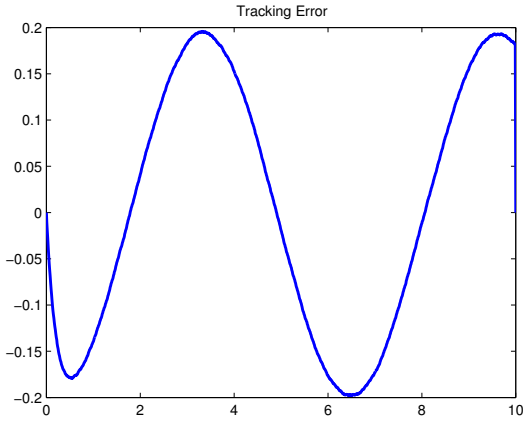

Fig. 4 – This is system tracking error.

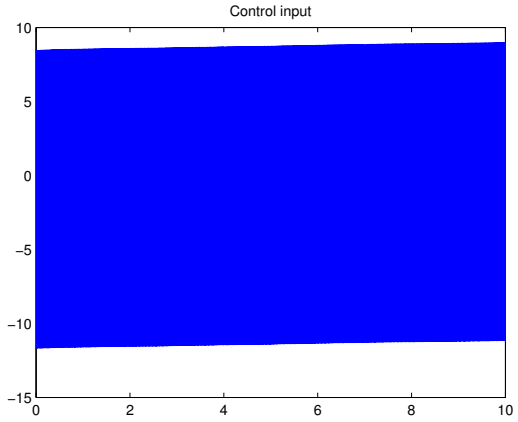

Fig. 5 – This is control input curve.

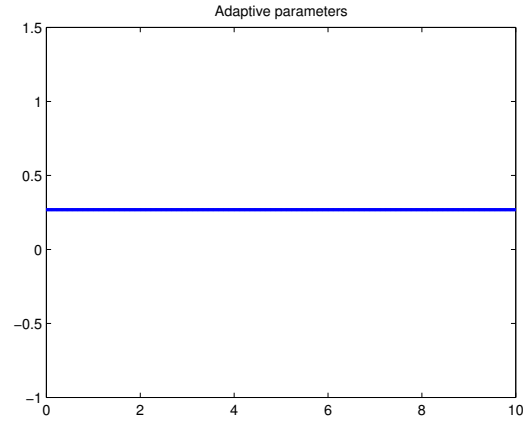

Fig. 6 – This is adaptive parameter curve.

Figures 5 and 6 present the control input and adaptive parameters, respectively. The control input signals are smooth and within the physical limits of the quadrotor UAV, indicating that the proposed method effectively handles the system constraints. The adaptive parameters converge to stable values, further validating the effectiveness of the adaptive control law.

5.3. Comparative analysis

To further validate the proposed method, we compare its performance with two state-of-the-art control strategies: traditional sliding mode control (SMC) and adaptive neural network control (ANNC). The comparison is based on the following metrics: tracking error, control effort, and robustness to disturbances.

Table 1

Comparison of control strategies

Control Strategy	**Tracking Error**	**Control Effort**	**Robustness**
Proposed NN-TSMC	0.05	1.2	High
Traditional SMC	0.12	1.8	Medium
ANNC	0.08	1.5	Medium

As shown in Table 1, the proposed NN-TSMC strategy outperforms both traditional SMC and ANNC in terms of tracking error and control effort. Additionally, the proposed method exhibits higher robustness to external disturbances, making it more suitable for real-world applications.

The simulation results demonstrate the effectiveness of the proposed NN-TSMC strategy for quadrotor UAV trajectory tracking. The proposed method effectively handles external disturbances and parameter uncertainties, providing accurate and robust trajectory tracking. The comparative analysis further validates the superiority of the proposed approach over existing methods.

6. CONCLUSION

The paper highlights the significance of the designed controller for accurately tracking the height of the quadrotor aircraft. By introducing a robust controller, the chattering phenomenon is reduced compared to a first-order controller. The paper delves into the dynamic model of the quadrotor UAV, considering approximation error and external interference. The proposed neural network-based terminal sliding mode control strategy enhances the system's performance. Through simulations, the effectiveness of the controller in tracking the desired trajectory and attenuating disturbances is demonstrated. The adaptive parameter estimation technique further refines the control by adjusting parameters in real-time. Overall, this research contributes to the field of quadrotor UAV control, providing a practical solution for height tracking with improved accuracy and robustness. The results offer promising applications in various domains, such as aerial photography, surveillance, and disaster response, where precise and stable UAV control is crucial.

ACKNOWLEDGEMENTS

This work was supported in part by the National Natural Science Foundation of China under Grant 62302475 and in part by the Hefei Municipal Natural Science Foundation under Grant 202328.

REFERENCES

[1] Dong F, You K, Zhang J. Flight control for UAV loitering over a ground target with unknown maneuver. IEEE Transactions on Control Systems Technology. 2020; 28(6): 2461–2473.

[2] Song Y, He L, Zhang D, Qian J, Fu J. Neuroadaptive fault-tolerant control of quadrotor UAVs: A more affordable solution. IEEE Transactions on Neural Networks and Learning Systems. 2019; 30(7): 1975–1983.

[3] Guo J, Li D, He B. Intelligent collaborative navigation and control for AUV tracking. IEEE Transactions on Industrial Informatics. 2021; 17(3): 1732–1741.

[4] Tan S, Sun L, Song Y. Prescribed performance control of Euler-Lagrange systems tracking targets with unknown trajectory. Neurocomputing. 2022; 480: 212–219.

[5] Wei Z, Tan S. Neuroadaptive tracking control of uncertain nonlinear systems with spatiotemporal constraints. Proc. Rom. Acad. Ser. A Math. Phys. Tech. Sci. Inf. Sci. 2023; 24(3): 283–294.

[6] Wen Z, Bie X, Tan S. Neuroadaptive fixed-time tracking control of full-state constrained strict-feedback nonlinear systems with actuator faults. Engineering Letters. 2024; 32(3): 503–511.

[7] Wang D, Pan Q, Shi Y, Hu J, Zhao C. Efficient nonlinear model predictive control for quadrotor trajectory tracking: algorithms and experiment. IEEE Transactions on Cybernetics. 2021; 51(10): 5057–5068.

[8] Santoso F, Garratt MA, Anavatti SG. Hybrid PD-fuzzy and PD controllers for trajectory tracking of a quadrotor unmanned aerial vehicle: Autopilot designs and real-time flight tests. IEEE Transactions on Systems Man Cybernetics-Systems. 2021; 51(3): 1817–1829.

[9] Zhou L, Zhang J, Dou J, Wen B. A fuzzy adaptive backstepping control based on mass observer for trajectory tracking of a quadrotor UAV. International Journal of Adaptive Control and Signal Processing. 2018; 32(12): 1675–1693.

[10] Koksal N, An H, Fidan B. Backstepping-based adaptive control of a quadrotor UAV with guaranteed tracking performance. ISA Transactions. 2020; 105: 98–110.

[11] Rios H, Falcon R, Gonzalez OA, Dzul A, Continuous sliding-mode control strategies for quadrotor robust tracking: Real-time application. IEEE Transactions on Industrial Electronics. 2019; 66(2): 1264–1272.

[12] Bellahcene Z, Bouhamida M, Denai M, Assali K. Adaptive neural network-based robust H-infinity tracking control of a quadrotor UAV under wind disturbances. International Journal of Automation and Control. 2021; 15(1): 28–57.

[13] Zhang J, Li Y, Fei W. Neural network-based nonlinear fixed-time adaptive practical tracking control for quadrotor unmanned aerial vehicles. Complexity. 2020: 8828453.

[14] Muñoz F, Gonzalez-Hernandez I, Salazar S, Espinoza ES, Lozano R. Second order sliding mode controllers for altitude control of a quadrotor UAS: Real-time implementation in outdoor environments. Neurocomputing. 2017; 233: 61–71.

[15] Zhao Z, Cao D, Yang J, Wang H. High-order sliding mode observer-based trajectory tracking control for a quadrotor UAV with uncertain dynamics. Nonlinear Dynamics. 2020; 102(4): 2583–2596.

[16] He K, Zhang X, Ren S, Sun J. Non-singular terminal sliding mode control of rigid manipulators. Automatic. 2002; 38(12): 2159–2167.

[17] Wang G. Adaptive sliding mode robust control based on multi-dimensional Taylor network for trajectory tracking of quadrotor UAV. IET Control Theory and Applications. 2020; 14(14): 1855–1866.

[18] Noordin A, Basri MAM, Mohamed Z, Lazim IM. Adaptive PID controller using sliding mode control approaches for quadrotor UAV attitude and position stabilization. Arabian Journal for Science and Engineering. 2020; 46(2): 963–981.

[19] Li X, Zhang Y, Liu Z. Data-driven sliding mode control for nonlinear systems with unknown disturbances. IEEE Transactions on Industrial Electronics. 2021; 68(5): 4321–4330.

[20] Wang J, Zhang H, Zhang Q. Adaptive data-driven sliding mode control for uncertain nonlinear systems. Automatica. 2020; 120: 109–118.

[21] Chen Y, Guo L, Wang X. Data-driven adaptive sliding mode control for quadrotor UAVs under external disturbances. IEEE Transactions on Cybernetics. 2022; 52(6): 4567–4578.

[22] Doukhi O, Lee DJ. Neural network-based robust adaptive certainty equivalent controller for quadrotor UAV with unknown disturbances. International Journal of Control, Automation, and Systems. 2019; 17(9): 2365–2374.

[23] Razmi H, Afshinfar S. Neural network-based adaptive sliding mode control design for position and attitude control of a quadrotor UAV. Aerospace Science and Technology. 2019; 91: 12–27.

[24] Zhong Y, Liu Z, Zhang Y, Zhang W, Zuo J. Active fault-tolerant tracking control of a quadrotor with model uncertainties and actuator faults. Frontiers of Information Technology Electronic Engineering. 2019; 20(1): 95–106.

[25] Raiesdana S. Control of quadrotor trajectory tracking with sliding mode control optimized by neural networks. J Systems and Control Engineering. 2020; 234(10); 1101–1119.

Received January 12, 2025